Improved structure of vertical flow velocity distribution in natural rivers based on mean vertical profile velocity and relative water depth

S. Song, B. Schmalz and N. Fohrer

ABSTRACT

Logarithmic, power, and parabolic distribution laws were proven to be efficient for the prediction of vertical velocity distribution. Traditionally, the distribution formulas involve the friction velocity (u_*) and the depth (y) of the measurement point. The low availability of friction velocity and limitation of real water depth data hindered the promotion and comparison of the available flow velocity formulas. In this paper, we proposed a new formula structure adopting a relative flow velocity based on mean vertical velocity ($u/\bar{u}$) and dimensionless relative water depth (y/H). The observations showed the following. (1) The substitution of u_* and y with $u/\bar{u}$ and y/H were reliable and applicable. Parabolic logarithmic and power fitting curves worked well, with an error of 7%, 10%, and 11%, respectively. (2) In water depth direction, the predicted results of the middle depth of the vertical profiles tend to be more reliable and precise. The highest estimated error appeared in the area near the water surface. (3) Higher catchment slope resulted in larger coefficients and constants in logarithmic and power fitting. (4) In the rivers with higher width-to-depth ratio, the maximum profile velocity occurred closer to the water surface, and mean profile velocity tended to happen more at the bottom.

Key words | dimensionless flow velocity, dimensionless water depth, natural rivers, vertical flow velocity distribution

S. Song (corresponding author)
School of Geographic and Oceanographic Sciences,
Nanjing University,
Nanjing,
Jiangsu Province,
China
E-mail: ssong@hydrology.uni-kiel.de

B. Schmalz
Institute of Hydraulic and Water Resources Engineering,
Technical University of Darmstadt,
Darmstadt,
Germany

S. Song
B. Schmalz
N. Fohrer
Department of Hydrology and Water Resources Management,
University of Kiel,
Kiel,
Germany

INTRODUCTION

A recurring problem in hydraulic or hydrological research and engineering is the estimation of vertical flow velocity distribution in open channels under varying conditions (Samani & Mazaheri 2010; Zeng & Huai 2014; Wang et al. 2017). Many attempts have been made to express the flow velocity distribution mathematically and distribution functions have been proposed to describe velocity under different hydraulic conditions (Wiberg & Smith 1991; Wang et al. 1995; Zhu & Li 2009; Wang & Huai 2016). According to the analysis, parabola line, power and logarithmic distribution lines are usually used to describe the vertical flow velocity profile. Previous studies suggested that a vertical profile from laminar flow fits the parabola line better, while vertical profiles from turbulent flow fit the logarithmic distribution law more frequently (Bowers et al. 2012; Campagnolo et al. 2013). In rivers of high width-to-depth ratio, the vertical velocity tends to show an exponential or logarithmic distribution (Chen et al. 1999; Bergstrom et al. 2001). Due to the complexity of natural river bed and river cross-section conditions, measured vertical velocity profiles frequently show mixed characteristics of two or three distribution laws.

The logarithmic distribution law or so-called law of the wall was proposed by Von Kármán (1931). He stated that the average velocity of a turbulent flow at a certain point is proportional to the logarithm of the distance from that

point to the river bed or bank (Von Kármán 1931). This well-known logarithmic law for flow velocity distribution was considered to be a good approximation for the entire flow velocity profile of natural rivers and has been used widely in various turbulent shear flows over a solid surface, such as boundary layer flows, pipe flows, and open-channel flows (Cheng & Chiew 1998).

While there are several manifestations of the law of the wall, the most succinct one is as follows:

$$U^+ = \frac{1}{\kappa}\ln y^+ + B_i \qquad (1)$$

where $U^+ = u/u_*$, u is the mean point velocity, u_* is the friction velocity defined from the wall skin friction through its relationship with the stress at the bottom (τ_b), $u_* = \sqrt{\tau_b/\rho}$ (ρ is the density of the flow); $y^+ = y/y_0$, y is the distance between measured point and river bed; y_0 is the height at which $u = 0$; $y_0 = \nu/u_*$ under smooth walls condition (ν is the kinematic viscosity), and $y_0 = y_r$ under rough walls condition (y_r is the roughness height); κ is the so-called von Kármán constant and B_i is another constant.

During the last 80 years, the logarithmic distribution law has been extensively studied by engineers and researchers. A literature review shows that κ is considered to cover the range of 0.35–0.45 (Zagarola & Smits 1998; He & Wang 2003; Zanoun *et al.* 2003). The constant B_i was believed to be universal, but recent research showed that it covers a wide range from 4 to 10 (Perlin *et al.* 2005; George 2007).

Most of the k and B_i discussed in the literature are based on laboratory experiments or pipe flow data. Natural rivers have not been extensively analyzed as yet. One of the reasons is the difficulty of determining friction velocity u_* in non-uniform flow in the field because of the complexity of natural flow conditions (Wei *et al.* 2005; Alfredsson & Örlü 2012).

According to the principle of dimensional analysis, the power law was presented as an alternative model to represent the vertical distribution of velocity in open channel flows in the 1930s (Zhang & Dong 1998). It can be expressed, in general, as follows:

$$U^+ = c(y^+)^n \qquad (2)$$

where c is the constant and n is the index, and the other variables are the same as in the logarithm law (Formula (1)). The applicability of different power functions was analyzed by González *et al.* (1996). Both c and n are empirical constants that are determined by the specific hydraulic condition. The variation and complexity of the open flow lead to the lack of universality of the constants. The combination of $c = 8.74$ and $n = 1/7$ is far more common compared with other conditions (Zhang 2008). Based on the theoretical considerations, the perfect agreement between the power law and the logarithmic law requires that the product of k, c, and n should be equal to $1/e$ (e is the base of natural logarithms) (Chen 1991). Experimental research showed that for low Reynolds numbers in open channels, the power law seems to describe the velocity distribution better than the logarithm law in the boundary layer, and the power law provides a better estimation for u_* (Bergstrom *et al.* 2001).

The existence of the parabolic nature of flow velocity distribution of turbulence in open channels has been mentioned by earlier investigators (Blench 1966; Coleman 1973). Based on cross-sectional flow velocity data, experimental scientists put forward a parabolic law of water profile (Sarma *et al.* 1983), which can be explained as:

$$\frac{u_m - u}{u_*} = c\left(1 - \frac{y}{h}\right)^2 \qquad (3)$$

where u_m is the maximum point velocity along the vertical profile, c is a pending constant, y is the depth of the measured point from the bottom, and h is the real water depth of the profile. Observations later showed that the boundary between the inner and outer regions of the vertical flow profile, which is marked by y/h, is independent of the Reynolds number of flow (Vedula & Achanta 1985). New expressions of the parabolic distribution based on Formula (3) were established and certificated in a recent study (Zhang 2008).

In addition to these three main flow velocity distribution laws discussed above, more vertical profile description formulas were established based on theoretical assumptions, such as the quadratic polynomial distribution law and rectangular cross-sectional binary velocity distribution formulas (Coleman 1973; Guo 2014). Being expressed by the deduced parameters in a complex form, these new formulas

are inefficient in a wide application range because of the theoretical argument.

The logarithmic, power, and parabolic vertical velocity distribution laws mentioned in this paper involve u_*, which is difficult to measure directly. Calculated values of u_* based on different deduction methods were proven to be of less consistency (Zhang 2008). The absolute depths of the measured points in the logarithm law and the power law make the comparative analysis of the distribution law between different laboratory experiments and open flow data even more difficult. Consequently, the a priori Formulas (1)–(3) are with high uncertainty but widely adopted in velocity estimation. A formula involving easy-to-determine and dimensionless parameters, and despite being a posteriori from measurement, would be a good solution to the velocity estimation and the comparison among different sites. In this paper we take $u/\bar{u}$ ($\bar{u}$ is the mean profile velocity) and relative depth (y/h) as the dimensionless flow velocity and depth to search for a new distribution formula for vertical flow velocity profiles.

The objectives of the study are to analyze the vertical velocity distribution formula in natural rivers in various catchments based on the relative flow velocity and relative depth; specifically, we (1) evaluate the applicability of the three prediction curves by fitting the predicted velocity values against the real measured values from the field, (2) analyze the accuracy of the formulas at different relative depths, (3) identify where the maximum velocity and mean velocity are located in the profile and (4) discuss the value ranges of the formulas' coefficient in three catchments.

METHODOLOGY

Improved structure of vertical flow velocity distribution

Improved structures of logarithmic, power, and parabolic velocity distribution, Formulas (4)–(6), were set up based on the relative velocity and depth. To maintain the uniformity of the variables, instead of Formula (3), Formula (6) was taken to express the parabolic velocity distribution. Formula (6) was derived based on Formula (3) and was proven to be applicable in laboratory experiments (Yan *et al.* 2005). The three distribution laws were consequently transformed into

the following forms:

$$\frac{u}{\bar{u}} = k_1 \ln\left(\frac{y}{h}\right) + b_1 \tag{4}$$

$$\frac{u}{\bar{u}} = k_2 \left(\frac{y}{h}\right)^n \tag{5}$$

$$\frac{u}{\bar{u}} = k_3 \left(\frac{y}{h}\right)^2 + k_4 \left(\frac{y}{h}\right) + b_2 \tag{6}$$

where k_1, k_2, k_3, and k_4 are coefficients; n, b_1, and b_2 are constants, and the remaining symbols are the same as mentioned above.

Study area and the water profiles

FlowSens (SEBA Hydrometrie, Germany), ADC (Acoustic Digital Current Meter, OTT Company, Kempten/Germany), and Acoustic Doppler Qliner (ADQ, OTT Company, Kempten/Germany) are widely accepted for use in hydrodynamic sampling (Figure 1). The measurement principle, as well as the reliability and accuracy of results of this equipment, has been verified in earlier research (Frizell & Vermeyen 2007; Muste *et al.* 2008; Wu *et al.* 2011; Song *et al.* 2012).

The FlowSens and ADQ were used as complementary to each other in the field. The FlowSens was applied in the narrow shallow rivers or streams with heavy vegetation where the ADQ was not suitable, while the ADQ was preferred for the deep and fast flowing steams (OTT 2008; SEBA 2010). All the velocity profiles in the Chinese Changjiang catchment were measured with ADC. Field campaigns were accomplished from October 2010 to December 2011 in the Upper Stör (northern Germany), Kinzig (west-central Germany) and Changjiang catchment (China) to record the vertical water profiles (Table 1). Finally, 248 water profiles were measured in order to set up and verify our assumptions in Formulas (4)–(6). The characteristics of all three catchments are shown in Figure 2.

The upper Stör catchment is located in the middle of Schleswig-Holstein/Northern (Figure 2(a) and 2(b)). The area is dominated by shallow groundwater tables and glacial and glacifluvial sediments, and the landscape is mainly covered by arable land (48.1%), pasture (29.5%), and forest (9.1%) (Müller-Wohlfeil *et al.* 2000; Schmalz *et al.* 2008; Schmalz & Fohrer 2009). Stör catchment is part of the

Figure 1 │ Equipment used to sample the hydrodynamics in this study.

northern German lowland area and in most of the catchment the slope gradients are usually smaller than 1° in most parts of the catchment, except for the southwestern part, which has gradients of more than 3° (LVA 1995).

The Kinzig catchment lies between 15 and 80 km east of Frankfurt am Main in southeastern Hessen, Germany. The main river is 86 km long and drains a catchment of 1,059 km² (Figure 2(c) and 2(d)). The altitude of the catchment ranges from 627 m at origin down to 98 m in the Main valley (Meurer 2012). It is classified as a mid-sized

fine-to-coarse substrate dominated siliceous highland river (HMUELV 2011).

The Changjiang basin is situated in the southeast of China (Figure 2(e) and 2(f)). The catchment area is 1,700 km² and the main Changjiang stream drains into Poyang Lake. The landscape in the catchment is characterized by a hilly terrain with the highest peaks at the northern and northwestern catchment borders (Strehmel 2011). The highest point of the catchment is at an altitude of 1,699 meters (m.a.s.l.) while the catchment's outlet has an altitude of 57 m.a.s.l.

Table 1 │ Evaluation sites and the number of measurements

Catchment	Location	Size (km²)	Landscape type	Main river slope (%)	Width (m)	Depth (m)	No.[a]
Upper Stör	Schleswig-Holstein, Germany	468	Lowland	0.22	10–15	1.5–2.5	140
Kinzig	Hesse, Germany	1,059	Low mountain area	0.62	15–25	1–2	48
Changjiang	Anhui Province, China	1,700	Mountainous area	1.93	60	1–1.5	60

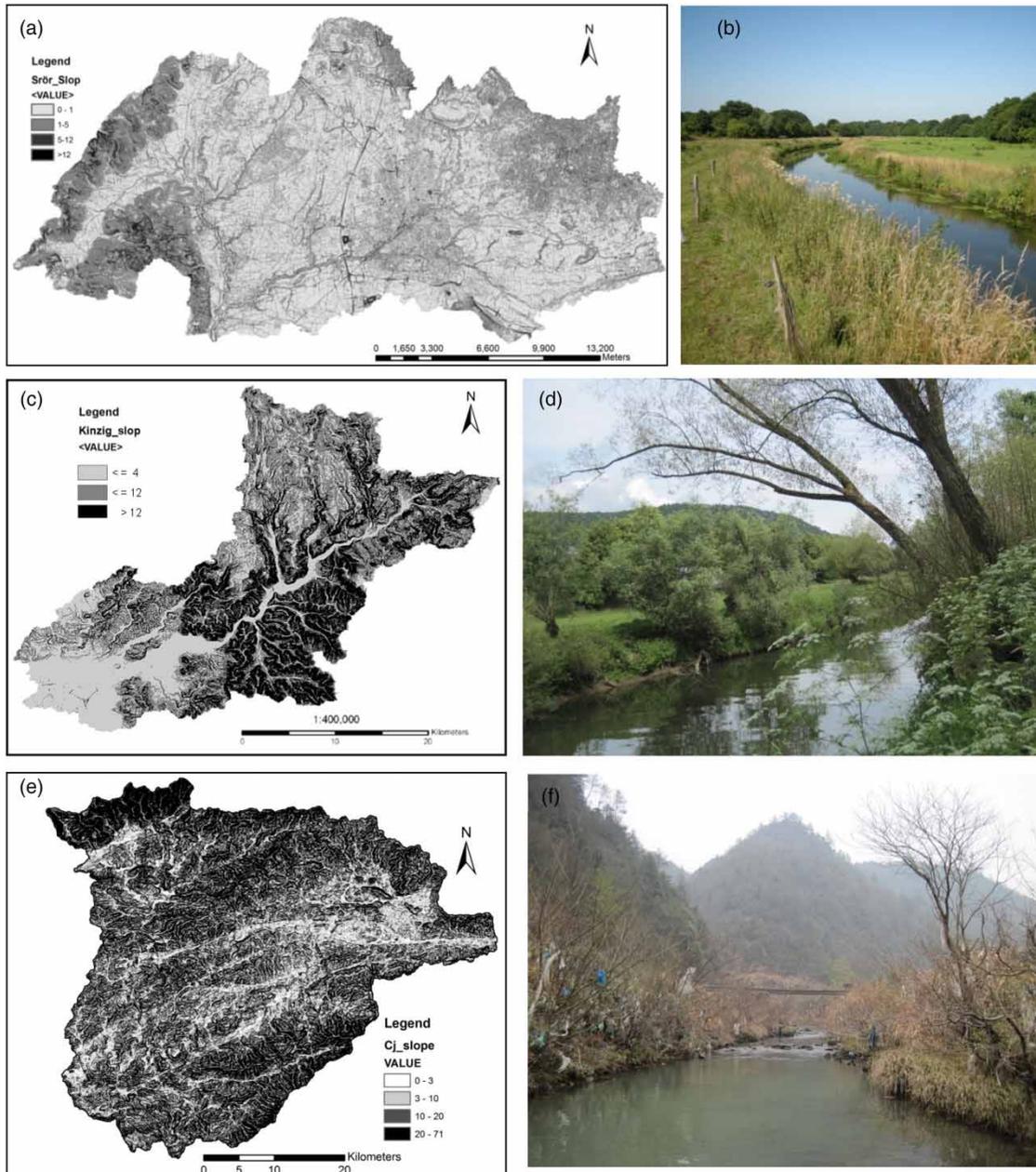[a]Number of the vertical water profile measurements.

Figure 2 | The slope maps and landscape photos of the studied catchments: (a) and (b) Upper Stör catchment (LVermGeoSH 1995); (c) and (d) Kinzig catchment (HVBG 2011); (e) and (f) Changjiang catchment (ISDSP 2013). Map created using ArcMap 10.2 software (Environmental Systems Resource Institute (ESRI), Redlands, CA, USA), http://www.esri.com/software/arcgis/arcgis-for-desktop.

STATISTICAL ANALYSIS

Fitting analysis of synthetic values against measured velocities

The logarithmic, power and parabolic synthetic velocities were fitted against the measured velocity of all three catchments. Coefficient of determination (R^2) and residual sum of squares (RSS) are representative indexes of regression quality. The cumulative probability distributions of R^2 of every vertical profile and the relative error of every single point were adopted to test the accuracy of the prediction formulas. Finally, a comparison analysis was made

between the coefficients and constants derived from each catchment to examine the complexity of the prediction formula.

Fitting results

Analysis of fitting results for logarithmic fitting, power curve, and parabolic curve resulted in R^2 higher than 0.75 and RSS less than 0.18. This demonstrates that all three curves can describe the vertical distribution in a satisfying way (Table 2).

The averaged R^2 of the 248 verticals fitting with Formulas (4)–(6) tends to be convincing, although the RSS and the coefficient of variation (CV) of these fitted vertical profiles showed high variability. According to R^2 and RSS of the fittings, the parabolic prediction showed the highest accuracy and the logarithmic fitting showed relatively higher accuracy than power fitting. Higher variability of parabolic formula parameters was indicated by the higher CV values of k_3, k_4, and b_2.

Correlation of fitted coefficients and constants

Fitting analysis revealed the high positive correlation between k_1 and b_1, and k_2 and n, while k_3 is strongly and negatively correlated with k_4 (Table 3). The correlation coefficients were 0.76, 0.73, and −0.94, respectively. The strong correlations provided the possibility of expressing constants with coefficients in Formulas (4)–(6).

In addition, k_2 is shown to be highly correlated with b_1 and the sum of parabolic coefficients and constant ($k_3 + k_4 + b_2$), with correlation coefficients of 0.70 and 0.77, respectively (Table 3). According to Formulas (4)–(6), when $y/h = 1$, the ratio of surface velocity to the profile averaged velocity can be expressed by b_1, k_2, and $k_3 + k_4 + b_2$. Consequently, these three parameters from the same vertical profile should be approximately equal to each, which is roughly the case of our study ($b_1 = 1.28$, $k_2 = 1.47$, and $k_3 + k_4 + b_2 = 1.1$, on average). Regression analysis between b_1, k_2, and $k_3 + k_4 + b_2$ reveals high agreement between the three data series. As shown in Figure 3, k_2 can be expressed

Table 2 | Averaged values of the results of logarithmic, power and parabolic fittings

Logarithmic			Power			Parabolic		
	Averaged	CV		Averaged	CV		Averaged	CV
R^2-L	0.77	0.28	R^2-P1	0.75	0.29	R^2-P2	0.78	0.33
RSS-L	0.18	1.09	RSS-P1	0.14	1.29	RSS-P2	0.11	1.35
k_1	0.5	0.55	k_2	1.47	0.33	k_3	−1.91	−1.1
						k_4	3.12	0.7
b_1	1.28	0.24	n	0.71	0.63	b_2	−0.11	−5.25

L, logarithmic fitting; P1, power curve; P2, parabolic curve.

Table 3 | Correlation coefficients of fitted parameters

Correlation coefficient	k_1	b_1	k_2	n	k_3	k_4	b_2	$k_3 + k_4 + b_2$
k_1	1.00							
b_1	**0.76**	1.00						
k_2	**0.73**	0.70	1.00					
n	0.61	0.16	**0.73**	1.00				
k_3	−0.22	−0.28	0.20	0.35	1.00			
k_4	0.51	0.49	0.09	−0.09	**−0.94**	1.00		
b_2	**−0.73**	−0.40	−0.29	−0.35	**0.69**	**−0.86**	1.00	
$k_3 + k_4 + b_2$	0.41	0.44	**0.77**	0.55	**0.70**	−0.45	0.22	1.00

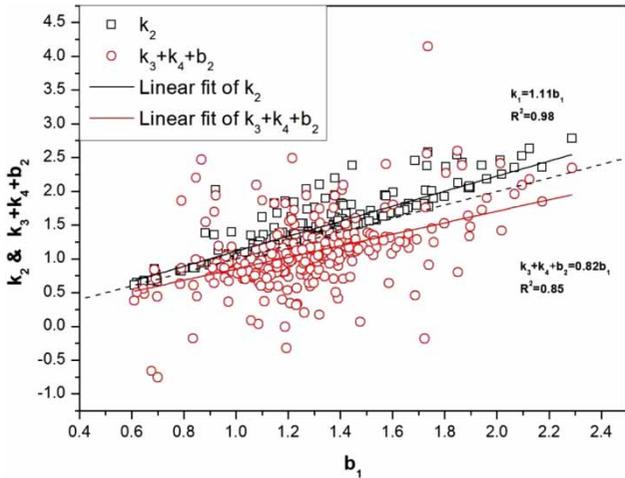*Note:* the bold, italic numbers refer to the relatively higher correlation of the two parameters.

Figure 3 | The relationship between b_1, k_2, and $k_3 + k_4 + b_2$. The dashed line represents the ideal $y + x$ line.

as $1.11b_1$, with R^2 of 0.98, while $k_3 + k_4 + b_2$ can be expressed by $0.82b_1$, with R^2 of 0.85.

The linear fitting between fitted coefficients and constants was done to explain their algebraic relationship

(Figure 4(a)–4(c)). The R^2 of the fitting was 0.89, 0.84, and 0.90, respectively. The regression formulas demonstrated that b, n, and k_4 can be approximately expressed as $2.25\,k_1$, $0.47\,k_2$, and $-1.26\,k_3$.

Accuracy of the prediction at different measured water depths

Relative error of the single points at different depths

As is shown in Figure 5, the highest error of the logarithmic prediction formula was at the water surface area, where the real measured velocity was higher than the fitted velocity by 15%. Near the river bottom the error was ±5–10%. In the middle parts, the deviations of the fitted values from the measured values were within a range of ±5%, which reveals high quality of the logarithmic prediction especially in the middle part of the verticals.
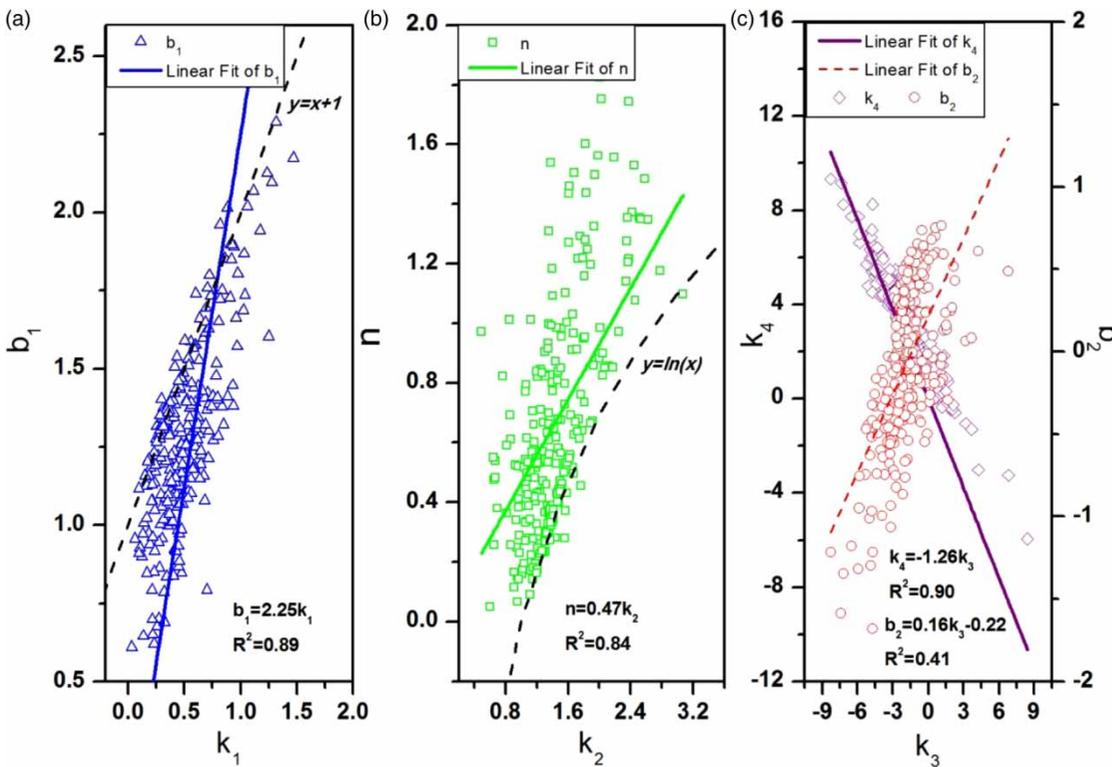

Figure 4 | Linear fitting of fitted coefficients and constants: (a) logarithmic fitting; (b) power fitting; (c) parabolic fitting. The dashed line in (a) and (b) represents the ideal relationship when the averaged velocity occurs at the relative depth of $1/e$; e is the base of the natural logarithm.
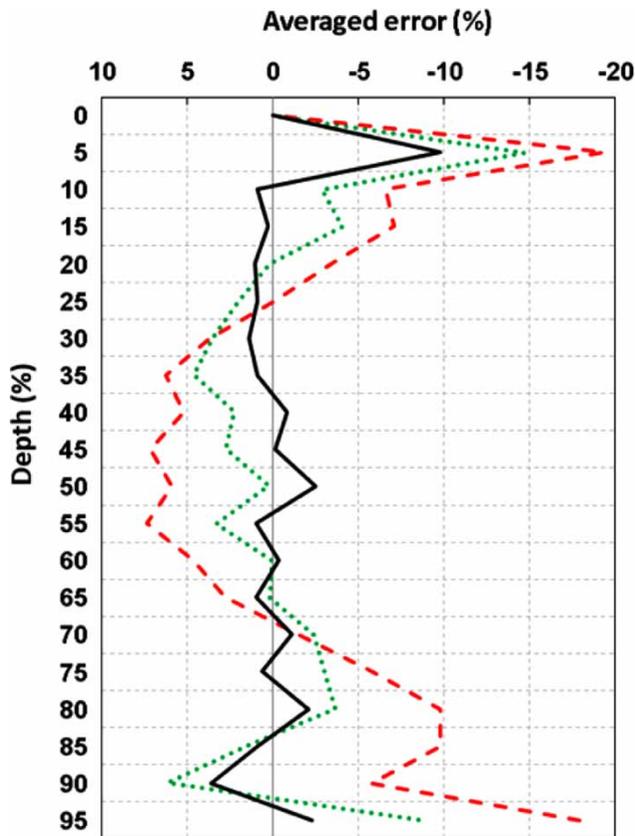
Figure 5 │ Averaged error of every single point velocity at different relative depths. *Note:* dotted line is the error of logarithmic curve; dashed line and black solid line represent the error of power and parabolic fitting, respectively.

Figure 5 also clearly shows that the errors of the power fitting were as high as −20% near the river surface and bottom. The power synthetic velocity from the river bed to around two-thirds of the water depths was about 10% lower than the real measured values. A similar phenomenon was observed near the water surface area. The measured values were higher than the fitted velocities by around 5% in the middle part of the profiles. Generally speaking, the synthetic velocity was smaller in the lower and upper water layers, while in the middle layer the fitted velocities were higher than the observations.

Although the averaged error suggested that the parabolic curve estimated the vertical velocity with the highest quality, the high estimated error at the water surface area was still as high as −10%. Apart from that, the prediction agreed well with the measured field data in the other parts of the profile.

Averaged absolute relative error of single points at different depths

Figure 6 displays the averaged absolute error of the synthetic point velocity to the measured point velocity at every measured point in water depth direction. The higher deviation trend in the water surface and bottom area is shown by the lines. All the averaged absolute errors were smaller than 20%, which means that the three curves performed well in the whole profile. The averaged absolute errors were 10%, 11%, and 7% for logarithmic, power, and parabolic fitting, respectively. In accordance with the results of the averaged error analysis, the highest deviation from the measured velocity appeared at the area near the water surface. The errors reached 17%, 20%, and 13% in the logarithmic, power, and parabolic prediction, respectively. Close to the river bed, absolute error of the power function
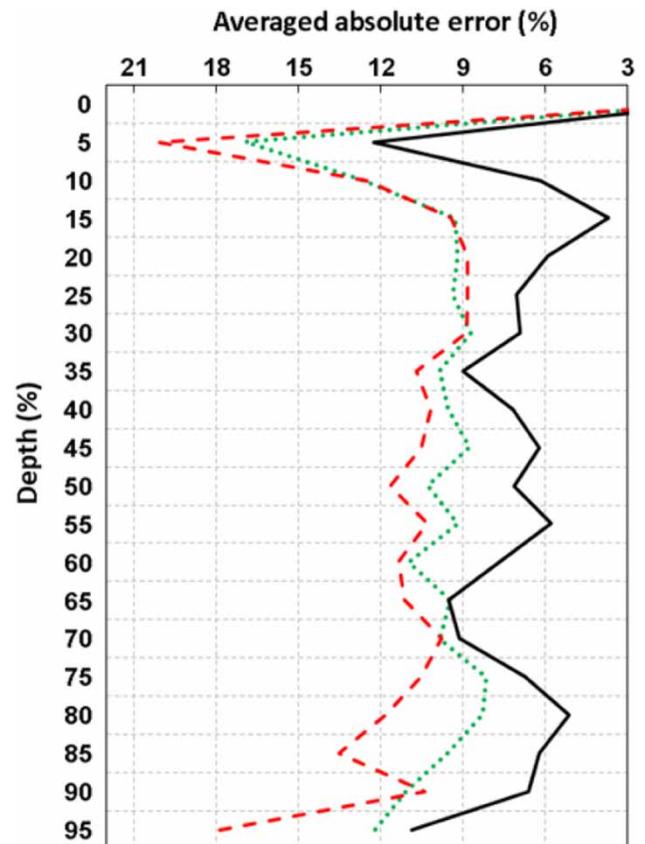

Figure 6 │ Averaged absolute error of every single point velocity at different relative depths. *Note:* dotted line is the absolute logarithmic error; dashed line and black solid line represent that of power and parabolic fitting, respectively.

was as high as 18%, and the absolute errors of logarithmic and parabolic formulas were around 10%. In the middle part of the profile, the absolute error of the logarithmic fitting ranged from 4% to 10%, while the power and parabolic fitting results deviated more than 10% from the real measured data.

Variability of fitted parameters in different catchments

Logarithmic fitting

Logarithmic fitting analysis indicated that the coefficient k_1 ranged from 0.25 to 1.5, and constant b varied from 0.5 to 2.5 from all the fitting profiles. The box plots of k_1 and b_1 in Figure 7 revealed a similar degree of dispersion, but different value ranges in Stör, Kinzig, and Changjiang catchments. In the Stör catchment, k_1 varied from −0.4 to 1.3 with an average value of 0.37, while the k_1 value in the

Kinzig catchment increased overall and reached an average value of 0.63. Compared with the condition in the Kinzig catchment, the k_1 value range of the Changjiang catchment increased and the averaged value was as high as 0.75. This implied that the vertical velocity in the Changjiang catchment tended to increase faster from the bottom to the water surface.

The constant b_1 of the three catchments showed similar trends. The Changjiang catchment provided the highest value range with the average value of 1.50. The averaged b_1-Kinzig and b_1-Stör are 1.28 and 1.19, respectively. This demonstrated the higher surface velocity in the craggy catchment.

Power fitting

Figure 8 presents the box plots of the power fitted coefficients and indices. The coefficient k_2 ranged from 0.4 to
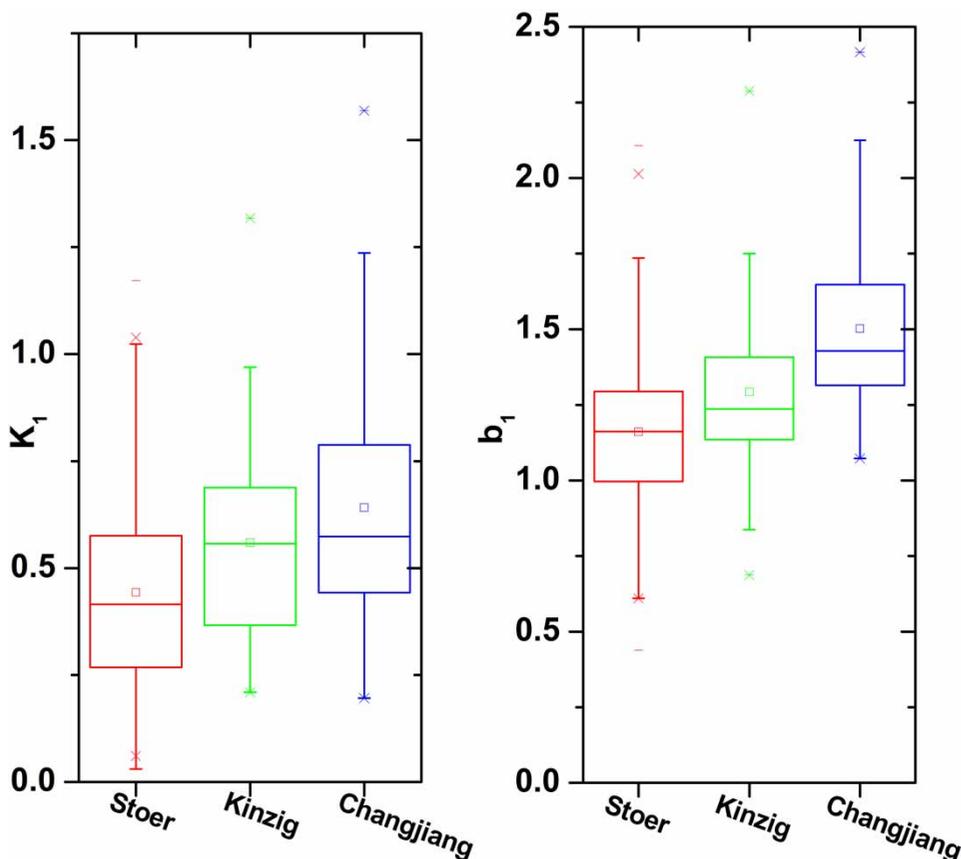

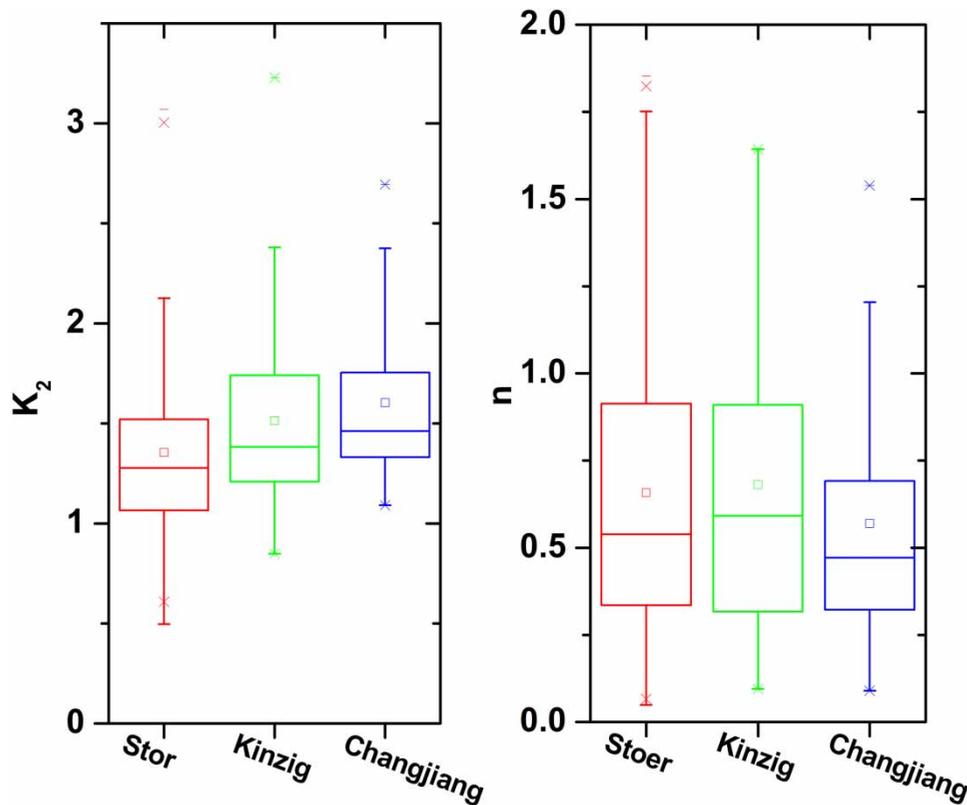**Figure 7** │ Box plot of k_1 and b in different catchments.

Figure 8 │ Box plots of the coefficient k_2 and index n in different catchments.

3.4, while the index n varied from -0.6 to 1.8, which implies a similar variability to that of the logarithmic parameters. The figure also shows that the distributions of k_2 and n in the Changjiang catchment were relatively more centralized compared with those of the other two catchments. Apart from that, the increasing tendency of k_2 with the increase of the catchment slope was revealed. No noticeable difference of n was discovered except for its lower dispersion in the Changjiang catchment. The averaged n values in the three catchments were around 0.52 and very close to each other. The higher coefficients in the steeper catchment manifested the higher surface velocity and steeper vertical velocity profiles.

Parabolic fitting

The box plot of the parabolic parameters in Figure 9 shows that there is considerable scatter in the coefficients k_3 and k_4. However, in spite of this scatter, it is also readily apparent that the parameters from Kinzig catchment had the widest

value ranges, while the Changjiang catchment parameters displayed the lowest dispersion. In addition to the individual parameters, the sum of k_3, k_4, and b_2 was further explored based on the fact that this sum is the ratio of the surface velocity to the profile averaged velocity. The increase of this sum value in Kinzig and Changjiang catchments clarifies the higher ratio between surface velocity and profile averaged velocity in mountainous catchments. This is consistent with the results of the logarithmic and power fittings.

DISCUSSION

Formula parameters

Parabolic fitting leads to the highest regression quality between measured and fitted data with the highest R^2 and lowest RSS, but the higher CV of k_3, k_4, and b_2 suggests that they are sensitive to the channel hydrological conditions, such as roughness, width-to-depth ratio, river
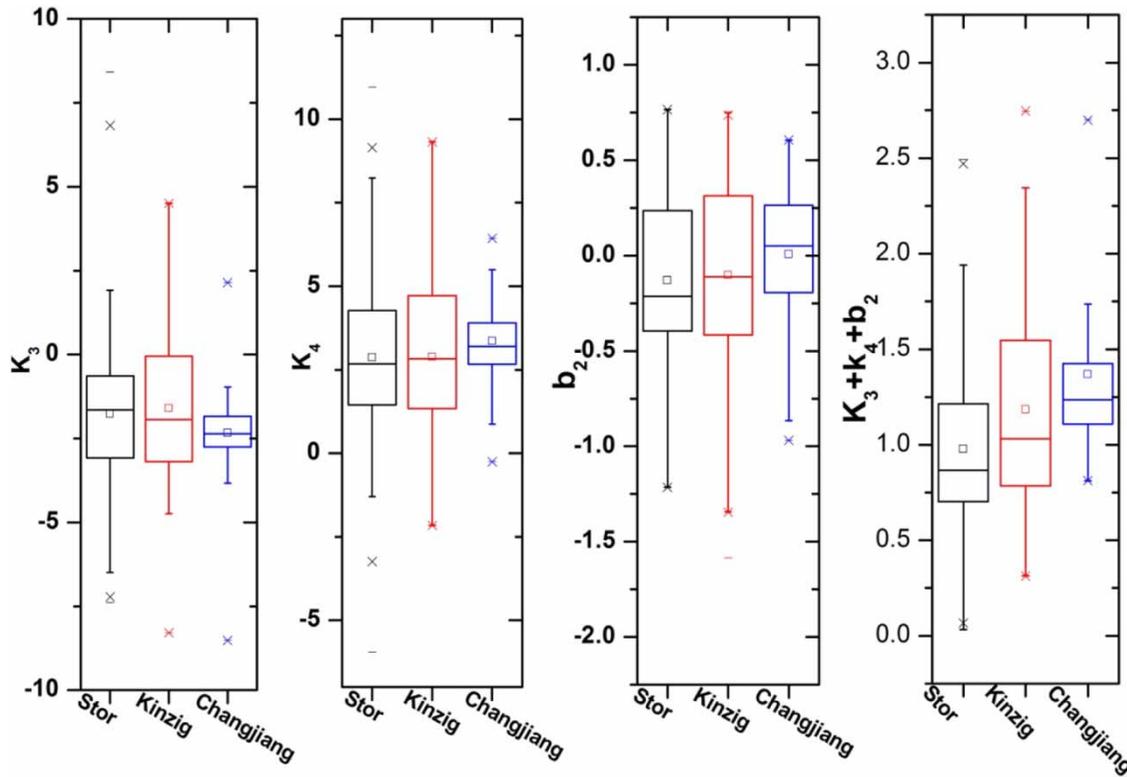
Figure 9 │ Box plots of the parabolic parameters in different catchments.

slope, etc. The logarithm formula and power formula provided similar fitting quality, but the higher index variability in power fitting made the logarithmic formula relatively superior. It is difficult to find the unique coefficients and constants that are applicable for natural rivers within the same catchment or among the different catchments.

This is consistent with the fact that the vertical water profiles in the natural rivers demonstrate logarithmic, power, and parabolic characteristics simultaneously (Afzal 2001). Due to the complexity of geometry, boundary resistance, and other hydraulic or hydrological factors, the idea of a universal law for flows is not supported by either the theory or the data (George 2007; Huai *et al.* 2009a, 2009b). However, the high correlation between the fitted coefficients and constants provided the opportunity to establish the simplified but relatively rough formulas.

Prediction and relative depth

All three prediction formulas worked well in the whole water profile with averaged error around ±10%. The

averaged error and the averaged absolute error of the profile at the different relative depths of the profile proved that the parabolic fitting provides the best quality in describing the vertical velocity distribution, while the power fitting leads to the highest prediction errors. The quality of the logarithmic prediction was in between the power and parabolic fitting at nearly all relative depths. Earlier researchers also pointed out that parabolic fitting was most appropriate for describing the vertical water profile in natural rivers or channels (Sarma *et al.* 1983; Zhang 2008). In addition, previous studies mentioned that the verticals in wide and shallow rivers with larger width-to-depth ratio tended to display exponential or logarithmic characteristics (Chen 1991; Bergstrom *et al.* 2001). However, the rivers in our study had a relatively low width-to-depth ratio, which might explain the higher efficiency of the parabolic prediction.

Prediction in different catchments

The fitted coefficients and constants varied in a wide range both within the same catchment and

among the different catchments, which leads to inefficiency in the setup of the uniform formula. Generally speaking, the increase of the logarithmic coefficient (k_1) and constant (b_1) with the rise of the river slope represents the steeper vertical water profiles. Although the index (n) valued around 0.52 and varied slightly among different catchments, the power coefficient (k_3) rises apparently from the lowland area to the mountainous catchment.

Despite the considerable scatter of the parabolic coefficients (k_3 and k_4), the sum of the parabolic coefficients and constants (b_2) explained the greater increase rate of velocity from bottom to the surface of the mountainous vertical water profiles. Coincidentally, the variability of parabolic fitted coefficients and constants between different rivers was even higher according to some previous literature (Sun *et al.* 2004).

Mean velocity, maximum velocity and relative depth

The relative depths where the maximum and mean profile velocity occur (*RD-max* and *RD-mean*) were recognized based on the measured profile velocity, and the effect of width-to-depth ratio was analyzed (Figure 10(a)). With the increase of width-to-depth ratio, the maximum velocity tended to occur at a higher relative depth, while the mean profile velocity was, on the other hand, inclined to appear on the lower part of the profile. In our study area, the averaged width-to-depth ratios of the three study areas were 10 (Upper Stör), 22 (Kinzig), and 75 (Changjiang), and *RD-max* of each was 0.71, 0.73, and 0.80, respectively (Figure 10(b)). This can be explained by the higher shear stress to the water body in the rivers with lower width-to-depth ratio. The averaged *RD-means* of the Upper Stör and Kinzig catchments were similar, 0.45 and 0.46.
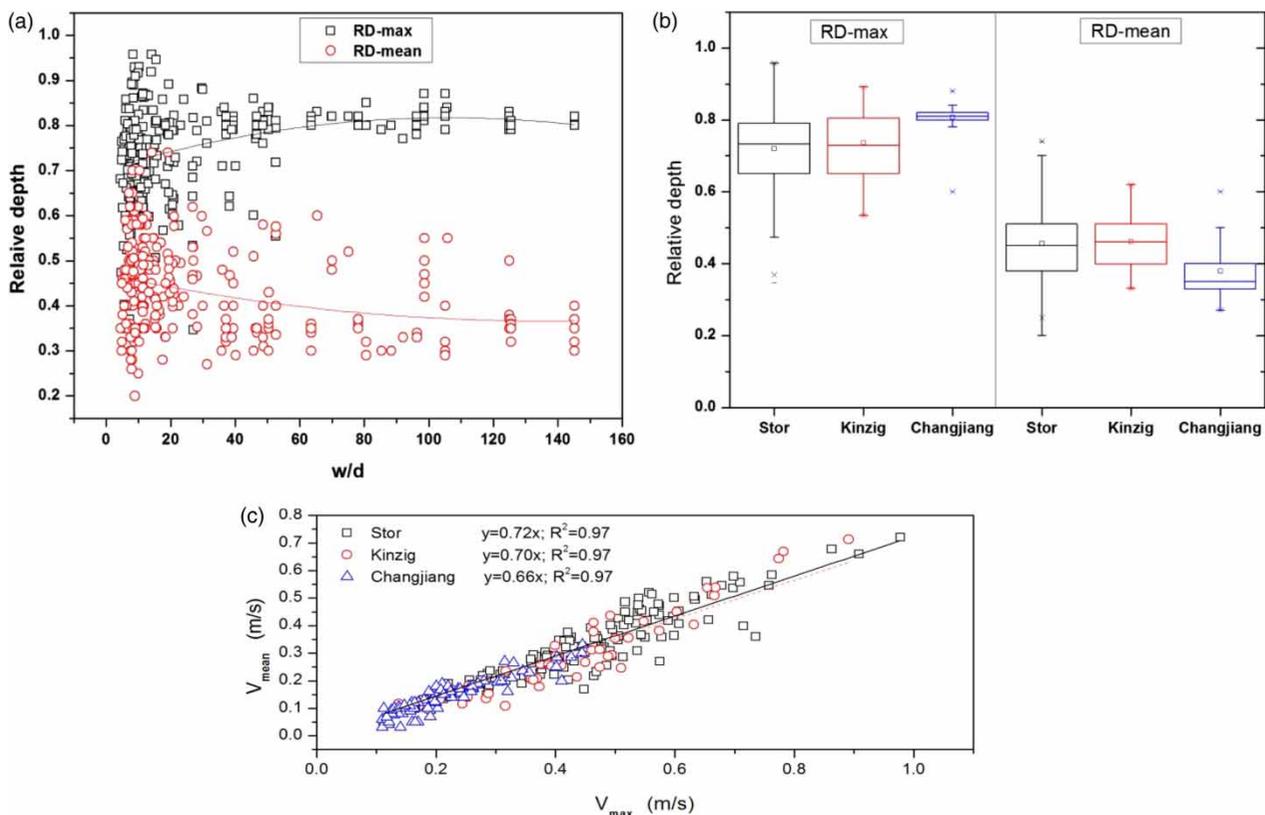

Figure 10 │ The relative depth at which maximum profile velocity and mean profile velocity occur: (a) the effect of w/d to maximum and mean profile velocity; (b) comparison between the catchments; (c) the ratio of mean profile velocity and maximum point velocity. Note: *RD-max* refers to the relative depth of maximum profile velocity and *RD-mean* refers to relative depth where the mean profile velocity occurs. w/d represents width-to-depth ratio; the black solid line is the fitting line of V_{mean}/V_{max} in the Upper Stör catchment, while the dashed line and dotted line represent that in Kinzig and Changjiang catchments, respectively.

In Changjiang catchment, the averaged *RD-mean* was 0.38, very close to the $1/e$ ($1/e \approx 0.37$) in the ideal profile. This seems to imply that the natural velocity profile occurs when the width-to-depth ratio is high enough. In addition, both value ranges of *RD-max* and *RD-mean* were on declining trends in rivers with high width-to-depth ratio.

The mean value of the ratio of the mean and maximum velocities of flow in a channel section is constant (Chiu & Said 1995). Here, we plot the ratio of mean velocity and maximum velocity in Figure 10(c). According to the figure, the mean velocity was around 0.72 times the maximum velocity in the Upper Stör catchment, while the fitting slope in Kinzig and Changjiang catchments was 0.70 and 0.66, respectively. Accurate estimation of mean profile velocity based on the maximum velocity, or vice versa, can be achieved.

CONCLUSION

Based on the dimensionless relative flow velocity and relative water depth, the three vertical velocity distribution predicting formulas were set up. Empirical analysis with 248 vertical water profiles measured from a northern German lowland catchment, a low mountain catchment in southern Germany, and a mountainous catchment from China reached the following results:

(1) The logarithmic, power, and parabolic formulas described the vertical distribution at a precise level. The parabolic formula provided the best prediction, while the logarithmic formula tended to be slightly superior to the power formula. The substitution of U^+ and y^+ in the old formulas with the relative flow velocity $u/\bar{u}$ and relative depth y/h were proven to be reliable and applicable.

(2) In the vertical direction, all three prediction formulas showed highest deviation in the area near the water surface. Apart from that, the predicted errors in the region near the river bed were also very high. The prediction for the middle part of the profile tended to be more reliable and precise.

(3) The variation of the formula coefficients and constants leads to the inefficiency in the setup of a uniform formula. The increases of the k_1, b_1, k_3 and the sum of the parabolic parameters ($k_3 + k_4 + b_2$) with the increase

of the catchment slope represent the greater velocity increase rate from the river bottom to the surface in steeper catchments. Despite the highest fitting quality of the parabolic formula, the scatter of fitted coefficients and constants was extremely large.

(4) With the increase of the width-to-depth ratio, the maximum profile velocity occurred at higher relative depth, while the mean profile velocity tends to appear at lower relative depth.

The logarithmic, power, and parabolic formulas discussed in this study proved the high reliability of substitution with $\bar{u}$ in vertical profile prediction. This then provides the opportunity to predict the whole vertical profiles with only $\bar{u}$ and the water depth. Combined with the mean profile velocity horizontal distribution prediction research, the point velocity distribution model for the whole cross section can be established and the required input for the model will be the geometry of the cross section and the experienced coefficients of the river section, which would be easily estimated with some real measured data. This model would generate a velocity data field with acceptable accuracy, which can then be linked to nutrient or pollution diffusion and transmission models to improve the simulation resolution.

REFERENCES

Afzal, N. 2001 Power law and log law velocity profiles in turbulent boundary-layer flow: equivalent relations at large Reynolds numbers. *Acta Mech.* **151**, 195–216. doi:10.1007/BF01246918.

Alfredsson, P. H. & Örlü, R. 2012 A new way to determine the wall position and friction velocity in wall-bounded turbulent flows. In: *Progress in Turbulence and Wind Energy IV, Springer Proceedings in Physics* (M. Oberlack, J. Peinke, A. Talamelli, L. Castillo & M. Hölling, eds). Springer, Berlin Heidelberg, pp. 181–185.

Bergstrom, D. J., Tachie, M. F. & Balachandar, R. 2001 Application of power laws to low Reynolds number boundary layers on smooth and rough surfaces. *Phys. Fluids 1994-Present* **13**, 3277–3284. doi:10.1063/1.1410383.

Blench, T. 1966 Discussion of 'Sediment transportation mechanics: initiation of motion'. *J. Hydraul. Div. ASCE* **92**, 287–288.

Bowers, M. C., Tung, W. W. & Gao, J. B. 2012 On the distributions of seasonal river flows: lognormal or power law? *Water Resour. Res.* **48**. doi:10.1029/2011WR011308.

Campagnolo, L., Nikolić, M., Perchoux, J., Lim, Y. L., Bertling, K., Loubiere, K., Prat, L., Rakić, A. D. & Bosch, T. 2013 Flow profile measurement in microchannel using the optical feedback interferometry sensing technique. *Microfluid. Nanofluidics* **14**, 113–119.

Chen, C. 1991 Unified theory on power laws for flow resistance. *J. Hydraul. Eng.* **117**, 371–389. doi:10.1061/(ASCE)0733-9429(1991)117:3(371).

Chen, S., Xiao, G., Zhao, Y., Zhang, J. & Wang, W. 1999 Study on velocity distribution function of river cross section. *J. Hydraul. Eng. Chin.* **4**, 70–74 (in Chinese).

Cheng, N. & Chiew, Y. 1998 Modified logarithmic law for velocity distribution subjected to upward seepage. *J. Hydraul. Eng.* **124**, 1235–1241. doi:10.1061/(ASCE)0733-9429(1998)124:12(1235).

Chiu, C.-L. & Said, C. A. A. 1995 Maximum and mean velocities and entropy in open-channel flow. *J. Hydraul. Eng.* **121**, 26–35.

Coleman, N. 1973 The velocity defect law and the sediment transfer coefficient in an open channel. *Proceedings, IAHR, International Symposium on River Mechanics, Sediment Transportation* **1**, 317–323.

Frizell, K. W. & Vermeyen, T. B. 2007 Comparing Apples and Oranges: Teledyne/RDI StreamPro ADCP and the OTT QLiner River Discharge Measurement System [WWW Document]. http://www.usbr.gov/pmts/hydraulics_lab/pubs/PAP/PAP-0965.pdf (accessed 17 February 2014).

George, W. K. 2007 Is there a universal log law for turbulent wall-bounded flows? *Philos. Trans. R. Soc. Math. Phys. Eng. Sci.* **365**, 789–806. doi:10.1098/rsta.2006.1941.

González, J. A., Melching, C. S. & Oberg, K. A. 1996 Analysis of open-channel velocity measurements collected with an Acoustic Doppler Current Profiler. In: *Proceedings from the 1st International Conference on New/Emerging Concepts for Rivers*, 22–26 September, Chicago, IL, pp. 838–845.

Guo, J. 2014 Modified log-wake-law for smooth rectangular open channel flow. *J. Hydraul. Res.* **52**, 121–128. doi:10.1080/00221686.2013.818584.

He, J. & Wang, H. 2003 Turbulence characteristics of non-uniform flow in a smooth open channel. *J. Hohai Univ. Nat. Sci.* **31**, 513–517 (in Chinese).

HMUELV 2011 Hessisches Ministerium für Umwelt, Energie, Landwirtschaft und Verbraucherschutz 2011 Beseitigung von kommunalen Abwässern in Hessen, Lagebericht 2010. Hessian Ministry of the Environment, Energy, Agriculture and Consumer Protection 2011 Disposal of Municipal Sewage in Hesse, Report 2010.

Huai, W., Han, J., Zeng, Y., An, X. & Qian, Z. 2009a Velocity distribution of flow with submerged flexible vegetations based on mixing-length approach. *Appl. Math. Mech.* **30**, 343–351. doi:10.1007/s10483-009-0308-1.

Huai, W. X., Zeng, Y. H., Xu, Z. G. & Yang, Z. H. 2009b Three-layer model for vertical velocity distribution in open channel flow with submerged rigid vegetation. *Adv. Water Resour.* **32**, 487–492. doi:10.1016/j.advwatres.2008.11.014.

HVBG 2011 *Hessische Verwaltung für Bodenmanagement und Geoinformation: Digitales Geländemodell [The Hessian State Office for Land Management and Geo-Information: Digital Elevation Model (DEM)]*.

ISDSP 2013 *International Scientific Data Service Platform: 30 m Resolution Digital Elevation Model*.

LVA, S.-H. 1995 *Digitales Geländemodell DHM50 für Schleswig-Holstein, Gitterweite 50 × 50 m [Digital Elevation Model DEM50 for Schleswig-Holstein, spatial resolution 50 × 50 m]*.

LVermGeoSH 1995 *Landesamt für Vermessung und Geoinformation Schleswig-Holstein (1995), Digitales Geländemodelle 1 (DGM 1) [State Office for Surveying and Geoinformation Schleswig-Holstein (1995), Digital Elevation Model DEM1]*.

Meurer, J. 2012 Modeling the Impact of Climate Change on Hydrology and Sediment Balance in a Low Mountain Range River Basin. Master Thesis, University of Kiel, Kiel.

Müller-Wohlfeil, D.-I., Bürger, G. & Lahmer, W. 2000 Response of a river catchment to climatic change: application of expanded downscaling to northern Germany. *Clim. Change* **47**, 61–89. doi:10.1023/A:1005613306339.

Muste, M., Kim, W. & Fulford, J. M. 2008 *Developments in Hydrometric Technology: New and Emerging Instruments for Mapping River Hydrodynamics*. World Meteorological Organization, Geneva.

OTT 2008 *ADC White Paper*. OTT Hydrometry Ltd, Sheffield.

Perlin, A., Moum, J. N., Klymak, J. M., Levine, M. D., Boyd, T. & Kosro, P. M. 2005 A modified law-of-the-wall applied to oceanic bottom boundary layers. *J. Geophys. Res. Oceans* **110**. doi:10.1029/2004JC002310.

Samani, J. & Mazaheri, M. 2010 An analytical model for velocity distribution in transition zone for channel flows over inflexible submerged vegetation. *J. Agric. Sci. Technol.* **11**, 573–584.

Sarma, K., Lakshminarayana, P. & Rao, N. 1983 Velocity distribution in smooth rectangular open channels. *J. Hydraul. Eng.* **109**, 270–289. doi:10.1061/(ASCE)0733-9429(1983)109:2(270).

Schmalz, B. & Fohrer, N. 2009 Comparing model sensitivities of different landscapes using the ecohydrological SWAT model. *Adv. Geosci.* **21**, 91–98.

Schmalz, B., Tavares, F. & Fohrer, N. 2008 Modelling hydrological processes in mesoscale lowland river basins with SWAT – capabilities and challenges. *Hydrol. Sci. J.* **53**, 989–1000. doi:10.1623/hysj.53.5.989.

SEBA 2010 *Mobile Discharge Measurement in Rivers, Channels, Sewer Flow, Fresh-, Waste- and Saline Water*. SEBA Hydrometrie, Germany.

Song, S., Schmalz, B., Hörmann, G. & Fohrer, N. 2012 Accuracy, reproducibility and sensitivity of acoustic Doppler technology for velocity and discharge measurements in medium-sized rivers. *Hydrol. Sci. J.* **57**, 1626–1641.

Strehmel, A. 2011 *Model-based Hydraulic Analysis of Flow and Sediment Transport in the Changjiang Basin in the Poyang Lake Region, China*. University of Kiel, Kiel, Germany.

Sun, D., Wang, E., Dong, Z. & Li, G. 2004 Discussion and application of velocity profile in open channel with rectangular cross-section. *J. Hydrodyn. Chin.* **19**, 144–151 (in Chinese).

Vedula, S. & Achanta, R. 1985 Bed shear from velocity profiles: a new approach. *J. Hydraul. Eng.* **111**, 131–143. doi:10.1061/(ASCE)0733-9429(1985)111:1(131).

Von Kármán, T. 1931 *Mechanical Similitude and Turbulence.* National Advisory Committee for Aeronautics, Washington, DC.

Wang, Y. & Huai, W. 2016 Estimating the longitudinal dispersion coefficient in straight natural rivers. *J. Hydraul. Eng.* **142**, 4016048.

Wang, X. J., Milner, T. E. & Nelson, J. S. 1995 Characterization of fluid flow velocity by optical Doppler tomography. *Opt. Lett.* **20**, 1337–1339. doi:10.1364/OL.20.001337.

Wang, Y.-F., Huai, W.-X. & Wang, W.-J. 2017 Physically sound formula for longitudinal dispersion coefficients of natural rivers. *J. Hydrol.* **544**, 511–523. doi:10.1016/j.jhydrol.2016.11.058.

Wei, T., Schmidt, R. & McMurtry, P. 2005 Comment on the Clauser chart method for determining the friction velocity. *Exp. Fluids* **38**, 695–699. doi:10.1007/s00348-005-0934-3.

Wiberg, P. L. & Smith, J. D. 1991 Velocity distribution and bed roughness in high-gradient streams. *Water Resour. Res.* **27**, 825–838. doi:10.1029/90WR02770.

Wu, N., Schmalz, B. & Fohrer, N. 2011 Distribution of phytoplankton in a German lowland river in relation to environmental factors. *J. Plankton Res.* **33**, 807–820. doi:10.1093/plankt/fbq139.

Yan, J., Wang, E., Sun, D. & Dong, Z. 2005 Experiment study velocity distribution characteristics in rectangular cross-section. *Eng. J. Wuhan Univ.* **38**, 58–60 (in Chinese).

Zagarola, M. V. & Smits, A. J. 1998 Mean-flow scaling of turbulent pipe flow. *J. Fluid Mech.* **373**, 33–79.

Zanoun, E.-S., Durst, F. & Nagib, H. 2003 Evaluating the law of the wall in two-dimensional fully developed turbulent channel flows. *Phys. Fluids 1994-Present* **15**, 3079–3089. doi:10.1063/1.1608010.

Zeng, Y. & Huai, W. 2014 Estimation of longitudinal dispersion coefficient in rivers. *J. Hydro-Environ. Res.* **8**, 2–8. doi:10.1016/j.jher.2013.02.005.

Zhang, X. 2008 Comparison and Study of the Open Channel Turbulent Velocity Distribution Formula. Master Thesis, Hohai University, China (in Chinese).

Zhang, Z. & Dong, Z. 1998 *Viscous Fluid Mechanics 358.* Tsinghua University Press, Beijing, China.

Zhu, C. & Li, S. 2009 Study on vertical velocity distribution with extra fine sediment. In: *International Conference on Test and Measurement, 2009. ICTM '09*, 5–6 December, Hong Kong, pp. 260–263. doi:10.1109/ICTM.2009.5413058.